Effect of Volume and Rate of Contrast Medium Injection on Intravenous Digital Subtraction Angiographic Contrast Medium Curves

FRED H. BURBANK, MD, WILLIAM R. BRODY, MD, PHD, BEVERLY R. BRADLEY, BS

Stanford, California

The image quality of temporal (mask mode) intravenous digital subtraction angiography is directly dependent on the shape of arterial time-concentration curves produced by the intravenous injection of contrast medium. Curves that are narrow and tall minimize motion artifact (misregistration) and maximize contrast enhancement (pre- and postcontrast differences).

To determine the effects of rate and volume of injection of contrast medium on intravenous digital subtraction angiographic curves, ioxaglate (Hexabrix), a monoacidic ionic dimer, was injected into large mongrel dogs. Quantitative measurements of opacification were made over time in the femoral arteries using a modified General Electric CT/T scanner. Peak opacification was directly proportional to the volume of contrast medium injected. Curve width was *not* affected by increasing volume of injection. At rates below a critical point, slower injection rates produced progressively shorter and wider arterial time-concentration curves. Above that critical point, increasing the rate of injection did not affect either curve width or curve peak.

Since 1897 when Stewart (1) described the first arterial time-concentration curve produced by injecting hypertonic saline solution, physiologists and cardiologists have extensively examined these curves (2–8). Area under the curve and mean transit time were of interest to these specialists because these variables could be related to cardiac output and central blood volume (9). For temporal (mask mode) intravenous digital subtraction angiography, the shape of the time-concentration curve produced by the intravenous injection of contrast medium is central. Tall curves maximize the difference between mask and contrast images. Narrow curves appear and disappear rapidly, minimizing the probability of motion artifact (misregistration) between mask and contrast images.

Intravenous digital subtraction angiography has evolved using central venous catheters, large volumes of contrast medium (30 to 60 ml/injection) and high injection rates (15 to 30 ml/s). The distribution of contrast medium has been examined in the past, but primarily over periods of minutes or hours (10–13) and not seconds. Burbank et al. (14) investigated the first pass kinetics of contrast medium, that is, the time when an intravenous digital subtraction angiographic image is produced, and showed that increasing the iodine content of contrast medium caused a proportionate increase in peak opacification. In addition, the biologic variables that determine curve peak and width were defined by Burbank (15). Curve peak is proportional to the milligram quantity of contrast medium iodine injected and inversely proportional to central blood volume. Curve width is proportional to central blood volume and inversely proportional to cardiac output. However, no prior study has systematically examined the effects of volume and rate of injection of contrast medium on arterial time-concentration curves. The goal of the present experiments was to determine the effects of varying the volume and rate of injection of contrast medium on time-concentration curve peak and width.

Methods

Experimental design. Five independent variables were studied in two separate research designs referred to as the "low rate" and the "volume-rate" experiments. *In the volume-rate experiment,* subject (dog) variability, injection se-

From the Department of Radiology, Stanford University School of Medicine, Stanford, California. This work was supported, in part, by funds from the Mallinckrodt Corporation, St. Louis, Missouri; Academic Training Grant HL-07425-02 from the National Institutes of Health, Bethesda, Maryland; Contract No. 1-HV-02922 from the National Heart, Lung, and Blood Institute, Bethesda, Maryland; the General Electric Company, Milwaukee, Wisconsin and the American Heart Association, Dallas, Texas. Dr. Brody is an Established Investigator of the American Heart Association. Manuscript received October 21, 1983; revised manuscript received February 28, 1984, accepted March 23, 1984.

Address for reprints: Fred H. Burbank, MD, Department of Radiology, Stanford University Medical Center, Room S056, Stanford, California 94305.

0735-1097/84/$3.00

Table 1. Volume-Rate Experimental Design (7 × 7 Greco-Latin square)

	Subject Number*													
	1		2		3		4		5		6		7	
Injection Sequence	Volume (ml)	Rate (ml/s)	Volume (ml)	Rate (ml/s)	Volume (ml)	Rate (ml/s)	Volume (ml)	Rate (ml/s)	Volume (ml)	Rate (ml/s)	Volume (ml)	Rate (ml/s)	Volume (ml)	Rate (ml/s)
1	20	12	12	10	16	18	8	14	14	16	10	6	18	8
2	12	18	16	14	8	16	14	6	10	8	18	12	20	10
3	16	16	8	6	14	8	10	12	18	10	20	18	12	14
4	8	8	14	12	10	10	18	18	20	14	12	16	16	6
5	14	10	10	8	18	14	20	16	12	6	16	8	8	12
6	10	14	18	16	20	6	12	8	16	12	8	10	14	18
7	18	6	20	8	12	12	16	10	8	18	14	14	10	16

*Each subject number represents a 70 minute experiment in one dog. During that session, seven injections of contrast medium were made at intervals of 10 minutes and assigned an injection sequence number from 1 to 7.

quence, volume of injection and rate of injection were studied. These variables were organized in a 7 × 7 Greco-Latin square (16). Table 1 presents the experimental design with the volume injected increasing from 8 to 20 ml and the rate of injection increasing from 6 to 18 ml/s. Seven dogs with an average weight of 37 kg were the experimental subjects. Theoretically scaling volume and rate of injection to a human subject weighing 70 kg, the volumes and rates ranged from 15 to 38 ml and 11 to 34 ml/s, respectively. The analysis of variance, least squares model describing the dependent variables assumes that each variable has a mean value, a subject effect, an injection sequence effect, a volume of injection effect, a rate of injection effect and an effect from random error.

In the low rate of injection experiment, subject (dog) variability, injection sequence, rate of injection and residual effects of sequential injection of contrast medium were studied. These variables were organized in a 6 × 6 extra period Latin square (17). Table 2 presents the experimental design with the volume of injection held constant at 14 ml (the average volume in the volume-rate experiment) and the rate of injection increasing from 1 to 10 ml/s. Six dogs with an average weight of 28 kg were the subjects. Theoretically scaling the rate of injection to a 70 kg human subject, the rates ranged from 2.5 to 25 ml/s. The analysis of variance, least squares model describing the dependent variables for the low rate experiment assumes that each dependent variable has a mean valve, a subject effect, an injection sequence effect, a rate of injection effect, an effect of each injection on the next injection and an effect from random error.

The dependent variables studied were the contrast medium time-concentration curve peak and width. The experimental data were used directly to define the peak. The downward sloping portion of the time-concentration curve, however, is distorted by recirculation, making measurement of curve width directly from the experimental data impossible. Time-concentration curve fitting can generate an idealized time-concentration curve, that is, one without recirculation (Fig. 1). Consequently, curve width was derived from gamma-variate curve fitting of each time-concentration

Table 2. Low Rate Experimental Design (6 × 7 extra period Latin square)

	Subject Number*											
	1		2		3		4		5		6	
Injection Sequence	Volume (ml)	Rate (ml/s)	Volume (ml)	Rate (ml/s)	Volume (ml)	Rate (ml/s)	Volume (ml)	Rate (ml/s)	Volume (ml)	Rate (ml/s)	Volume (ml)	Rate (ml/s)
1	14	10	14	8	14	6	14	4	14	2	14	1
2	14	6	14	4	14	2	14	1	14	10	14	8
3	14	8	14	6	14	4	14	2	14	1	14	10
4	14	2	14	1	14	10	14	8	14	6	14	4
5	14	1	14	10	14	8	14	6	14	4	14	2
6	14	4	14	2	14	1	14	10	14	8	14	6
7	14	4	14	2	14	1	14	10	14	8	14	6

*Each subject number represents a 70 minute experiment in one dog. During that session, seven injections of contrast medium were made at intervals of 10 minutes and assigned an injection sequence number from 1 to 7.

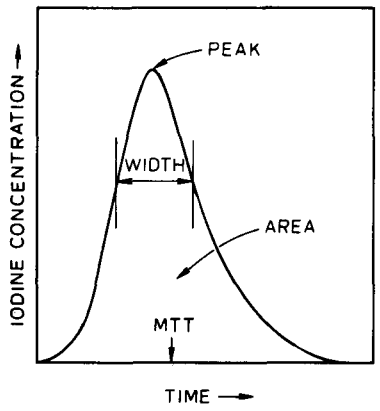

Figure 1. Cardiovascular variables from an idealized contrast medium gamma-variate time-concentration curve: peak (maximal iodine concentration), width (the interval between inflection points), mean transit time (MTT) (the time for half of the contrast medium dose to pass the X-ray detectors) and area under the curve.

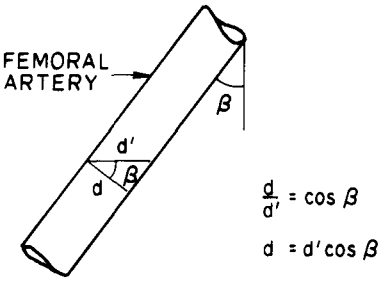

Figure 3. Trigonometry for measuring femoral artery diameter (d) when only the angle beta (β) and the length (d') can be observed directly.

curve and was defined as the interval between the first and second inflection points of the gamma-variate curve. The raw data collection rate was 15 points/s. Validation of the curve-fitting technique for iodinated contrast medium has been described (15).

X-ray technique. A noninvasive X-ray technique for in vivo quantitative measurement of contrast medium time-concentration curves was used (14). Briefly, the scanned projection digital radiography system consisted of a General Electric CT/T 8800 scanner modified to perform scanned projection radiography. In these studies, the X-ray tube emitted an 85 kVp beam at 1000 mA, pulsed at 15 Hz, with a pulse length of 3.3 ms. Each scan was 30 seconds in length. Counts of attenuated and unattenuated photons were digitized to 16 bit accuracy and transmitted to a Data General Corporation eclipse S/200 computer. Images were analyzed on a 320 × 320 pixel matrix video display. Resolution at the subject level was 0.55 mm/pixel. The scans were performed with the gantry and the table held stationary. Measurements were recorded in time at 15 Hz over the femoral arteries. Raw data were collected in opacification units. Opacification units were converted to contrast medium iodine concentration (mg I/ml) from the radiographic system calibration data and from measuring the diameter of the femoral arteries.

Validation of arterial diameter measurements. Because conversion from opacification units to chemical concentration units (mg I/ml) is directly dependent on arterial diameter measurement, a Plexiglas phantom with six

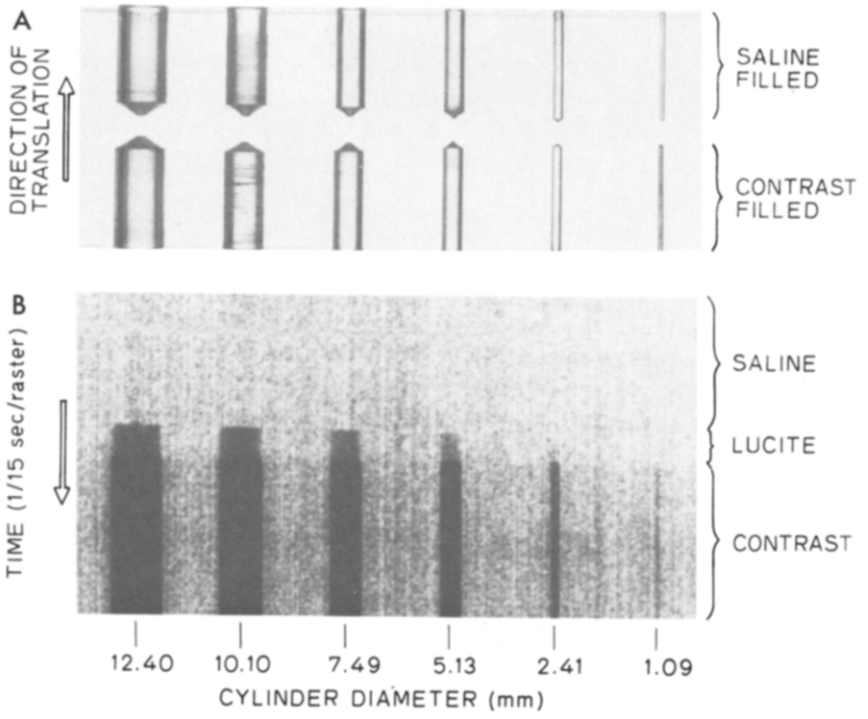

Figure 2. A, Plexiglas phantom used to estimate diameter measurement error; phantom was translated through the fan beam in the direction of the **arrow**. **B**, Line scan of phantom with anterior cylinders filled with saline solution and posterior cylinders filled with ioxaglate at 10 mg I/ml. CONTRAST = contrast scanned with saline subtraction; LUCITE = Lucite scanned with saline subtraction; SALINE = saline solution scanned with saline subtraction.

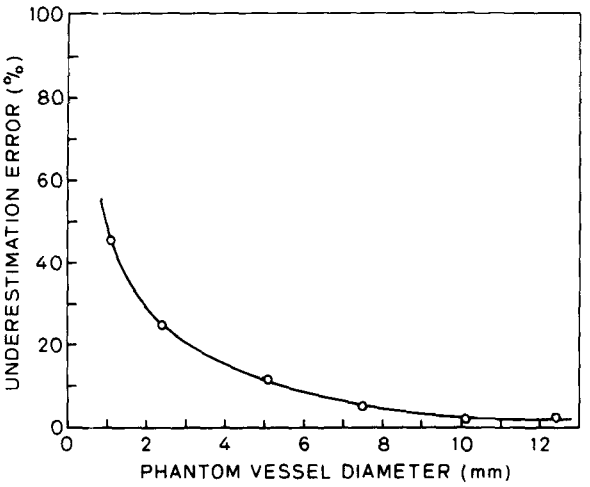

Figure 4. Phantom data showing increasing underestimate of vessel diameter with decreasing vessel diameter; the standard error of the mean for each mean value is smaller than the **open circles** in this figure.

pairs of holes varying from 1.1 to 12.4 mm in diameter was investigated (Fig. 2). The phantom (along with a calibration grid to correct for magnification) was translated through the X-ray fan beam, and the cylinder diameter was measured on the video display with a cross-hair cursor. The same subtraction algorithm used to create the experimental images from contrast medium passing through the femoral arteries was used to create the phantom images. Arterial diameter was measured by the same cross-hair cursor system.

Validation of volume and rate of injection. A power injector (Medrad IV) was used to deliver the volumes and the injection rates of the medium specified by both experimental designs. Because both experiments are highly dependent on the accurate delivery of the volume and rate of the contrast medium with each injection, the power injector performance was measured. Volumes delivered by the power injector were independently measured by quantitative analytic chemical methods. Rates of injection were validated using a timing strip recorder and a pressure transducer to determine the duration over which the power injector delivered each experimental volume at each rate setting. All injector validation measurements were performed through a 6F catheter, the same size catheter used for the experimental injections.

Experimental procedure. The dogs were anesthetized with pentobarbital, paralyzed with succinycholine and ventilated. They were apneic for the 30 second duration of each scan. Ioxaglate (Hexabrix) at a concentration of 320 mg I/ml was used for all injections. For the volume-rate experiment, the injection site was the subclavian vein. For the low rate experiment, contrast medium was injected into the right atrium. Scans were performed with the table and gantry held stationary, with line scan information collected over time. The scan line was approximately 2.5 cm below the dog's inguinal ligament. At the beginning of each session, a modified General Electric DF-3000 digital fluoroscope was used to obtain a standard digital subtraction angiogram of the femoral arteries and record the angle of the femoral artery at the level of the scan (Fig. 3 angle β). From the relation of the femoral artery angle (β) and the scan magnification, the diameter of the femoral artery (Fig. 3, d) was calculated from the line of opacification through the artery (Fig. 3, d').

Table 3. Diameter Phantom Data (contrast medium vessels all contained ioxaglate at 10 mg I/ml)

Micrometric Dowel Measurement (mm)*	Radiographic Measurement (mm)†	% Error
12.40	12.1 ± 0.01	2.4
10.10	9.9 ± 0.15	2.0
7.49	7.1 ± 0.10	5.3
5.13	4.5 ± 0.10	11.8
2.41	1.8 ± 0.10	25.0
1.09	0.6 ± 0.01	45.5

*Micrometric dowel measurements made to the nearest 0.001 mm; therefore, rounded to the nearest 0.01, these measurements have essentially no variability. †±SEM for n = 7; although cylinder diameter is underestimated, there is very little variability to the underestimate. The error, therefore, represents a consistent bias with a small random error.

These data show that as vessel diameter becomes small, radiographic diameter estimate error becomes very large.

Results

Validation of experimental measurements. Measurement of 10.1 and 12.4 mm phantom diameters was underestimated by only 2%. As diameters decreased, however, underestimation error increased (Table 3, Fig. 4). Even though small cylinder diameter was underestimated, the underestimate was consistent and predictable. At 2.41 mm, the radiographic estimate was 1.8 mm, a 25% underestimate; however, the standard error of the mean for seven observations was only 0.01 mm. The average arterial diameter observed radiographically over all contrast medium injections corresponded with an underestimation error of approximately 10%. Consequently, iodine concentration (mg I/ml) measurements were somewhat overestimated and cardiac output measurements were proportionately underestimated. Since the magnitude of error for these experiments was low, the data are presented without adjustment.

The power injector volumes and rates of injection correlated very closely with measured volumes and rates (Fig. 5). The volumes and rates specified in the experimental protocol were, therefore, delivered.

Quality of the experimental data. At the sampling rate employed (15 Hz), the raw data time-concentration curves were extremely smooth, defining peak iodine concentration

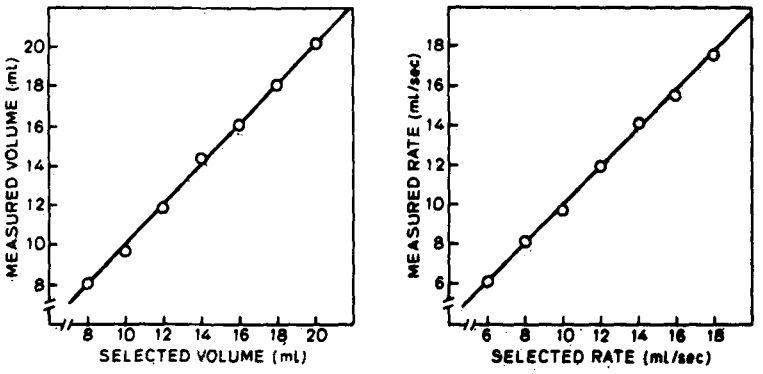

Figure 5. Left, Validation of volume injected by power injector, showing measured volume increasing as selected volume increases ($r = 0.99$, $p \leq 0.001$, slope = 1.02). **Right**, Validation of the rate of injection, showing measured rate increasing as the selected rate increases ($r = 0.99$, $p \leq 0.001$, slope = 0.96). The standard error of the mean for each mean value is smaller than the **open circles** in this figure.

of the contrast medium injected unambiguously in time and magnitude (Fig. 6). The gamma-variate curve fitting of the experimental data was very good, with a close correlation between the raw data and the gamma-variate fit variables and low root mean square error values (15).

Experimental effects. *Volume-rate experiments.* Peak iodine concentration increased in direct proportion to the volume of contrast medium injected (Fig. 7). Doubling the volume of injected contrast medium caused peak iodine concentration to double. Volume of injection, however, had no effect on curve width (Fig. 8.) Table 4 presents the analysis of variance for the curve peak. Volume of injection was the most influential independent variable on curve peak. Variation in the experimental subjects (dogs) was the next most influential variable. At rates of injection between 6 and 18 ml/s, rate of injection did not significantly influence curve peak. Table 5 presents the analysis of variance for curve width. Subject variability alone influenced width; volume and rate of injection had no effect.

Low rate of injection experiments. Rate of injection strongly influenced curve peak and width up to a cutoff point, approximately 7 ml/s (Fig. 9 and 10). The cutoff point will be referred to as the "distortion point" because injections performed at a rate below this point distort the shape of the time-concentration curves, creating curves that are no longer determined by quantity of contrast medium iodine injected, cardiac output and central blood volume. At a volume of injection of 14 ml, the distortion point corresponds to a duration of injection (the time the injector is on) of 2 seconds. With average curve widths of approximately 4 seconds, the distortion point appears to be that duration of injection which is approximately half the curve width. Below the distortion point, lower rates of injection produce time-concentration curves that are progressively shorter and wider.

Table 6 presents the analysis of variance for curve peak for the low rate experiment. At rates between 1 and 10 ml/s, rate of injection was the variable that most influenced

Figure 6. A typical time-concentration curve recorded during these experiments with the opacification index × 1,000 plotted as a function of time. Raw data are discrete points and show the beginning of recirculation. The gamma-variate curve fit of these raw data is a continuous line that has no recirculation and returns to the baseline.

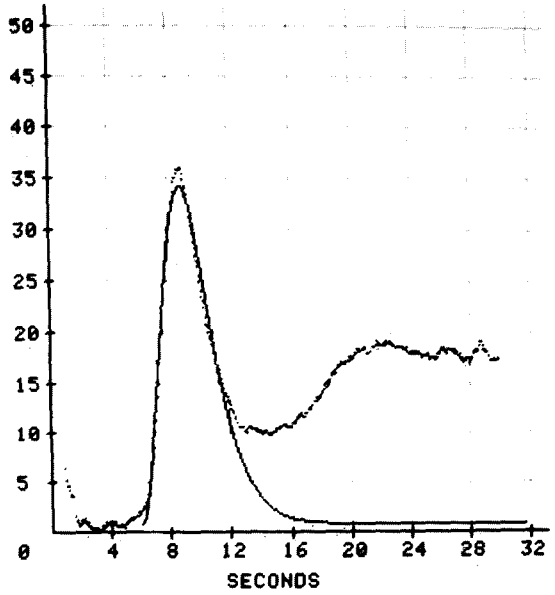

Figure 7. Volume-rate experimental data summarized by volume of injection, showing a linear increase in peak iodine concentration with increasing contrast medium volume ($r = 0.98$, $p \leq 0.001$, ± SEM, $n = 7$ each mean).

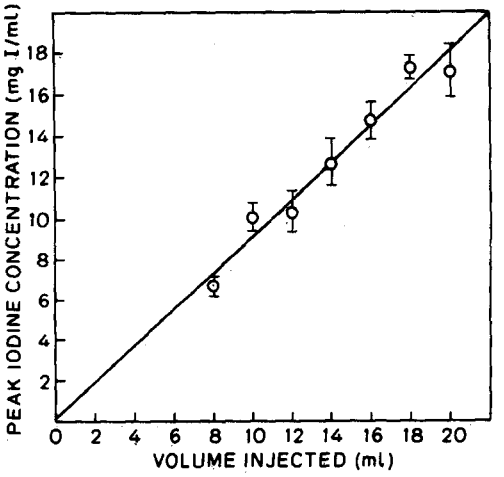

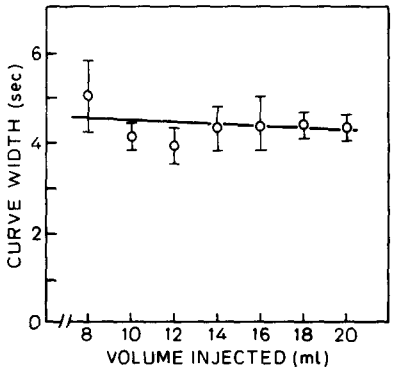

Figure 8. Volume-rate experimental data summarized by volume of injection showing *no significant effect* of increasing volume injected on time-opacification curve width (r = 0.25, ± SEM, n = 7 each mean).

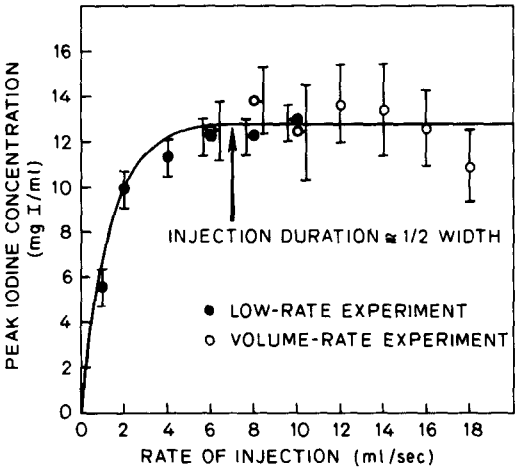

Figure 9. Volume-rate (**open circles**) and low rate (**solid circles**) experimental data adjusted for subject size and differences in site of injection, showing a decrease in curve peak as the rate of injection falls below the distortion point (injection duration approximately equal to half the curve width). Above the distortion point, increasing the rate of injection has no effect on curve peak. (± SEM, n = 7 each mean.)

curve peak. Subject variability (primarily variability in cardiac output and central blood volume) was the next most influential variable. The other variables (injection sequence and residual contrast medium effect) were not significant. Table 7 presents the analysis of variance for curve width for the low rate experiment. Rate of injection had the only significant influence on curve width.

Discussion

Increasing the volume of injection of contrast medium increases curve peak but does not affect curve width. It has been previously demonstrated (14) that peak opacification during intravenous digital subtraction angiography is proportional to the concentration of the contrast medium iodine injected. The current study demonstrates that peak opacification during intravenous digital subtraction angiography is also proportional to the volume of contrast medium injected (Fig. 7). For subclavian vein injections, equal degrees of opacification can be achieved by either increasing the concentration of the injectate at a fixed volume or increasing the volume at a fixed concentration (mg I = mg I/ml × ml). It is the milligram quantity of iodine injected that is important. When data from the current experiments

Table 4. Analysis of Variance for Curve Peak for the Volume-Rate Experimental Data

Source of Variance	Sum of Squares	Degrees of Freedom	Mean Square	F
Total	910	6		
Subject (dog)	135	6	22.6	8.7*
Injection sequence (period)	15	6	2.6	1.0
Volume	657	6	109.5	42.1*
Rate	40	6	6.6	2.5
Error	62	24	2.6	

*p ≤ 0.001. The rates of injection in this experiment fall along the "flat" portion of the curve in Figure 9.

Table 5. Analysis of Variance for Curve Width for the Volume-Rate Experimental Data

Source of Variance	Sum of Squares	Degrees of Freedom	Mean Square	F
Total	78			
Subject (dog)	56	6	9.4	23.9*
Injection sequence (period)	5	6	0.8	2.0
Volume	5	6	0.8	2.0
Rate	3	6	0.5	1.2
Error	9	24	0.4	

*p ≤ 0.001. The rates of injection in this experiment fall along the "flat" portion of the curve in Figure 10.

Table 6. Analysis of Variance for Curve Peak for the Low Rate Experimental Data

Source of Variance	Sum of Squares	Degrees of Freedom	Mean Square	F
Total	503.2	41		
Subject (dog)	159.1	5	31.8	9.2*
Injection sequence (period)	12.6	6	2.1	0.6
Residual effect	2.3	5	0.5	0.1
Rate	259.9	5	52.0	15.0*
Error	69.3	20	3.5	

*$p \leq 0.001$. The lowest rates of injection in this experiment fall along the "rising" portion of the curve in Figure 9.

Table 7. Analysis of Variance for Curve Width for the Low Rate Experimental Data

Source of Variance	Sum of Squares	Degrees of Freedom	Mean Square	F
Total	1817.9	41		
Subject (dog)	198.7	5	39.7	2.1
Injection sequence (period)	113.6	6	18.9	1.0
Residual effect	140.5	5	28.1	1.5
Rate	990.0	5	198.0	10.6*
Error	375.1	20	18.8	

*$p \leq 0.001$. The lowest rates of injection in this experiment fall along the "falling" portion of the curve in Figure 10.

are combined with data from prior experiments (14) and both sets of data are corrected for differences in subject weight, time-concentration curve peak is proportional to contrast medium load, mg I/kg (Fig. 11).

Burbank (15) demonstrated that time-concentration curve peak is proportional to the quantity (mg I) of contrast medium iodine injected and is inversely proportional to the central blood volume (approximately the volume of blood in the heart and lungs). Correcting for differences in subject (dog) weight roughly corrects for differences in central blood volume among the experimental subjects. With the variation in central blood volume corrected, peak iodine concentration

Figure 10. Volume-rate (**open circles**) and low rate (**solid circles**) experimental data adjusted for subject size and differences in site of injection, showing a rapid increase in curve width as the rate of injection falls below the distortion point (injection duration approximately equal to half the curve width). Above the distortion point, increasing the rate of injection has no effect on curve width. (± SEM, n = 7 each mean.)

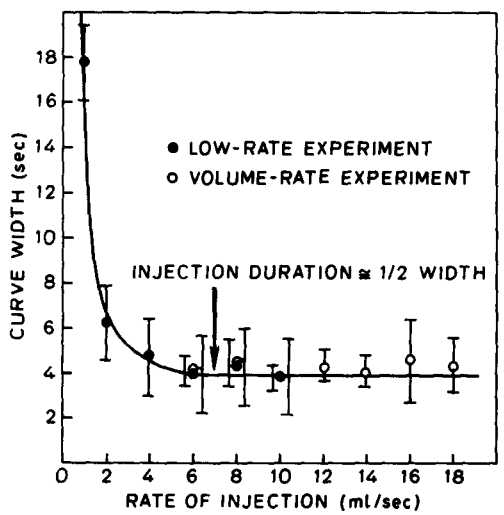

Figure 11. Volume-rate experimental data (**open circles**) and concentration experimental data (14) (**open squares**), showing a linear increase in peak iodine concentration with increasing contrast medium load (mg I/kg) produced by either greater volume or greater concentration of contrast medium injected ($r = 0.98$, $p \leq 0.001$).

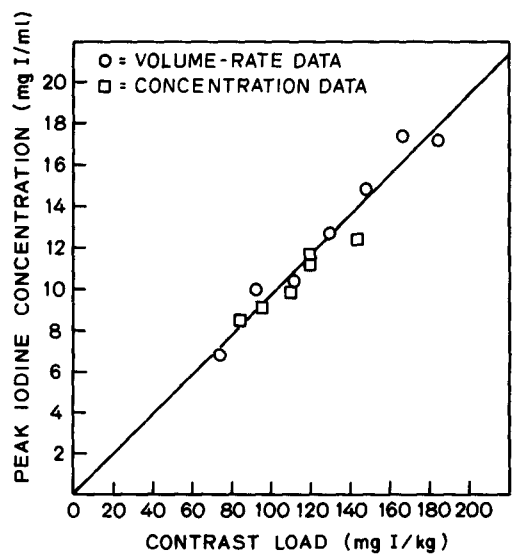

is proportional to the quantity of iodine injected. These findings suggest that subject size, along with estimates of the status of the cardiovascular system, should be taken into account when planning contrast medium dosages for intravenous digital subtraction angiography. Larger patients will need more contrast medium to achieve a given level of arterial opacification in an artery of given size; smaller patients will need less. Patients with congestive failure with a large central blood volume will require more contrast medium than size alone would predict.

Below a specific rate of injection (the distortion point), rate of injection affects both curve peak and width; above the distortion point, rate of injection has little or no effect. The rate of injection strongly affects peak and width of time-concentration curves when this rate is relatively slow. It is proposed that when the duration of injection (the time when the injector is on) is greater than approximately half a curve width, referred to as the distortion point, distorted time-concentration curves will be produced. In other words, the height and width of a curve produced below the distortion point will no longer be defined by the quantity of contrast medium iodine injected (mg I) and the biologic status of the subject (cardiac output and central blood volume) but will be additionally defined by the rate of injection. Alternatively, when the rate of injection is above the distortion point, the rate of injection will have no effect on curve peak or width.

Injection rates that are too rapid may produce suboptimal curves. One qualification, however, may be needed. At very high injection rates in relatively peripheral sites (for example, the subclavian vein), curve shape may be distorted secondary to partial peripheral reflux of contrast medium (for example, reflux up the jugular systems). Consequently, the low data point in curve peak seen in Figure 9 at 18 ml/s may be real (not just random variation) and may be caused by briefly overwhelming the flow capacity of the subclavian vein, causing reflux of contrast medium away from the heart. Very high injection rates in relatively peripheral sites may produce suboptimal contrast medium time-concentration curves. Once above the distortion point, increasing the injection rate does not improve the shape of the time-concentration curve. High injection rates do not produce tall narrow curves. Studying clinical material, Eskridge et al. (18) demonstrated that high injection rates do not improve the quality of intravenous digital subtraction angiographic curves as rated by clinical observer.

We thank Rupert Miller, PhD from the Department of Statistics, Stanford University, Stanford, California, for guidance before the experiments and for reviewing the manuscript.

References

1. Stewart GN. Researches on the circulation time and on the influences which affect it. J Physiol 1897–1898;22:159–83.
2. Stewart GN. The output of the heart of dogs. Am J Physiol 1921;57:27–50.
3. Stewart GN. The pulmonary circulation time, the quantity of blood in the lungs and the output of the heart. Am J Physiol 1921;58:20–44.
4. Kinsman, JM, Moore JW, Hamilton WF. Studies on the circulation. I. Injection method: physical and mathematical considerations. Am J Physiol 1929;89:322–30.
5. Moore JW, Kinsman JM, Hamilton WF, Spurling RG. Studies on the circulation. II. Cardiac output determination: comparison of the injection method with the direct Fick procedure. Am J Physiol 1929;89:331–9.
6. Hamilton WF, Riley RL, Attyah AM, et al. Comparison of the Fick and dye dilution methods of measuring the cardiac output in man. Am J Physiol 1948;153:309–21.
7. Hamilton WF, Moore JW, Kinsman JM, Spurling RG. Simultaneous determinations of the pulmonary and systemic circulation times in man and of a figure related to the cardiac output. Am J Physiol 1928;84:338–44.
8. Hamilton WF, Moore JW, Kinsman JM, Spurling RG. Studies on the circulation. IV. Further analysis of the injection method, and of changes in hemodynamics under physiological and pathological conditions. Am J Physiol 1931–1932;99:534–51.
9. Newman EV, Merrell M, Genecin A, Monge C, Milnor WR, McKeever WP. The dye dilution method for describing the central circulation. An analysis of factors shaping the time-concentration curves. Circulation 1951;4:735–46.
10. Cattell WR, Fry IK, Spencer AG, Purkiss P. Excretion urography. Factors determining the excretion of Hypaque. Br J Radiol 1967;40:561–80.
11. Leppits IE, Thompson CJ, Ethier R, Sherwin AL. Diatrizoate in computed cranial tomography: a quantitative study. Invest Radiol 1977;12:21–6.
12. Ono N, Martinez CR, Fara JW, Hodges FJ III. Diatrizoate distribution in dogs as a function of administration rate and time following intravenous injection. J Comput Assist Tomogr 1980;4:174–7.
13. Brennan RE, Rapoport S, Wernberg I, Pollack HM, Curtis JA. CT determined canine kidney and urine iodine concentrations following intravenous administration of sodium diatrizoate, metrizamide, iopamidol, and sodium ioxaglate. Invest Radiol 1982;17:95–100.
14. Burbank FH, Brody WR, Hall A, Keyes G. A quantitative in vivo comparison of six contrast agents by digital subtraction angiography. Invest Radiol 1982;17:610–6.
15. Burbank FH. Determinants of contrast enhancement for intravenous digital subtraction angiography. Invest Radiol 1983;18:308–16.
16. Bliss CI. Statistics in Biology, Statistical Methods for Research in the Natural Sciences; vol. 1. New York: McGraw-Hill, 1967:313–6.
17. Lucas HL. Extra-period latin-square change-over design. J Dairy Sci 1957;40:225–39.
18. Eskridge JM, Becker GH, Holden RW, et al. Digital vascular imaging: practical aspects. Radiology 1983;148:703–5.